Diluted Magnetic III-V Semiconductors

H. Munekata, H. Ohno,[a] S. von Molnar, Armin Segmüller, L. L. Chang, and L. Esaki
IBM T. J. Watson Research Center, P.O. Box 218, Yorktown Heights, New York 10598
(Received 8 August 1989)

A new diluted magnetic III-V semiconductor of $In_{1-x}Mn_xAs$ ($x \leq 0.18$) has been produced by molecular-beam epitaxy. Films grown at 300 °C are predominantly ferromagnetic and their properties suggest the presence of MnAs clusters. Films grown at 200 °C, however, are predominantly paramagnetic, and the lattice constant decreases with increasing Mn composition; both are indicative of the formation of a homogeneous alloy. These films have *n*-type conductivity and reduced band gaps.

PACS numbers: 75.50.Pp, 68.55.Bd, 73.60.Br

Diluted magnetic semiconductors are semiconductors in which a sizable fraction of the component ions are replaced by those of transition metals or rare earths, leading to a variety of cooperative effects. Most importantly, the state of magnetization changes the electronic properties (and vice versa) through the spin-exchange interaction between local magnetic moments and carriers.[1] Rare-earth and transition-metal chalcogenides have been the most widely studied magnetic semiconductors. For example, mixed crystals (alloys) can be formed over a wide range of compositions even if the crystal structures of the two component materials are different from each other, as exemplified by the ternary alloy $Cd_{1-x}Mn_xTe$. Among magnetic ions, many of the transition elements, particularly Mn^{2+} which tends to assume a spherically symmetric magnetic ground state, can be accommodated in the zinc-blende structure by substituting group-II cations in the II-VI compounds. In this paper, in contrast, we are concerned with the incorporation of high concentrations of magnetic ions in III-V compound semiconductors. Up to now, the number of magnetic ions incorporated in III-V semiconductors has been limited to doping levels 10^{18}–10^{19} cm^{-3},[2,3] beyond which surface segregation[4] and, in extreme cases, phase separation[5] occur and impede further incorporation of the magnetic ions into the crystals. These experiments imply that the preparation of ternary alloys to form diluted magnetic III-V semiconductors is an extremely difficult task. We consequently sought to study metastable solid phases using the diverse growth-parameter space provided by the molecular-beam-epitaxy technique. In this situation, the preparation of the material itself includes such fundamental subjects as solubility, stability of the resulting crystal structures, the valence state of the magnetic ions, and the associated magnetism, all of which are not usually encountered in isovalent semiconductor alloy systems.

Through the preparation and characterization of epitaxial films of InMnAs, we obtained experimental evidence for the formation of a III-V-based diluted magnetic semiconductor in which a large amount of Mn is incorporated at least up to an average composition of In/Mn/As = 0.82/0.18/1.0. Studying magnetic, metallurgical, and semiconducting properties, we find that the films may be classified into two different groups depending on the growth temperature. Films grown at relatively high temperatures (~300 °C) exhibit ferromagnetic behavior similar to that of MnAs which may exist in the form of clusters. Low-temperature growth (~200 °C), however, results in films where Mn is incorporated to form a homogeneous alloy; its paramagnetic behavior is evident from a Curie-Weiss law and its lattice constant changes monotonically with the Mn composition. The films exhibit *n*-type conduction and reduced band gaps compared to that of InAs. Multilayer structures of InAs/InMnAs were also successfully grown for both types of films. In addition, epitaxy of GaMnAs was similarly achieved at a growth temperature of 400 °C.

Films were grown by molecular-beam epitaxy on both InAs and GaAs(100) wafers, using elemental In, Mn, and As as source materials. Buffer layers of either InAs or GaAs were first grown under conventional growth conditions. Growth temperatures were 420° and 580 °C for InAs and GaAs layers with As-stabilized surfaces, respectively. This was followed by the deposition of InMnAs, where we found that the substrate temperature T_s strongly affected the deposition process. For T_s above ~400 °C, the deposition produced films which were porous and not adhered to the substrates. Reducing the temperature, however, resulted in epitaxy of InMnAs films as clearly observed in *in situ* reflection high-energy electron diffraction (RHEED). Films grown at T_s = 200°–300 °C proceeded with a twofold (2×1) RHEED pattern which lasted throughout the entire deposition up to a thickness of 3 μm without showing obvious signs of phase separation. At these growth conditions, the incorporation of Mn was controlled by simply varying the Mn beam flux while maintaining the In and As_4 beams constant. The As_4/In flux ratio was kept at ~6. The growth rates ranged from 183 Å/min for pure InAs to 225 Å/min for the film with a Mn composition of ~0.2. The films exhibited mirrorlike surfaces, and there was no sign of oxidation at atmospheric condition. Film compositions obtained from electron microprobe

analysis indicated a monotonic increase (decrease) of Mn (In) with increasing Mn beam flux, while retaining unity as the atomic ratio of the sum of In and Mn to As, as shown in Table I. Extending the epitaxial growth to the heterojunctions, we also found that single-crystal InAs layers can be grown on top of InMnAs surfaces without changing the substrate temperature of $T_s = 200°$-$300°$C. The twofold (2×1) RHEED pattern remained unchanged in transition from InMnAs to InAs and vice versa. This consequently led to the successful fabrication of InAs/InMnAs multilayer structures.

The magnetic properties of InMnAs films depend sensitively on the growth conditions. Figure 1(a) shows the temperature dependence of the magnetization in an applied magnetic field of $H_A = 20$ kOe for two 2.7-μm-thick InMnAs films grown on InAs(80 nm)/GaAs(100) at different substrate temperatures T_s. Both samples consisted of the same average composition of In/Mn/As $= 0.82/0.18/1.0$. The InAs buffer layers served the purpose of relaxing a large misfit strain between the GaAs substrates and the InMnAs films. Measurements were performed using a SQUID magnetometer for temperatures ranging from ~5 to 300 K. Two important conclusions may be drawn from the data in Fig. 1(a). The first is that both curves appear to consist of two components, one ferromagnetic and the other paramagnetic. The second is that whereas the $T_s = 300°$C sample is dominated by the ferromagnetic component, the $T_s = 200°$C sample clearly is primarily paramagnetic. To analyze these data we have assumed that the total magnetization $M_{\rm tot}$ may be written as

$$M_{\rm tot} = M_F(T) + \chi_p(T) H_A , \tag{1}$$

where $M_F(T)$ and $\chi_p(T)$ are the temperature dependences of the ferromagnetic component and the magnetic susceptibility of the paramagnetic component, respectively, and $\chi(T) = C/(T - \Theta_p)$, with C and Θ_p being a Curie constant and a paramagnetic Curie temperature. This separation may not be rigorously correct in view of the possibility that the effective field of the ferromagnetic component may necessitate correction to the second term of Eq. (1). Nonetheless, the two components may be separated by a linear extrapolation of the high-field data to $H_A = 0$.[6] For the $T_s = 200°$C sample, a plot of $[\chi_p(T)]^{-1}$ vs T derived in this manner is shown in Fig. 1(b). The ferromagnetic component in this sample represents only about 5% of the total Mn incorporated in the film.[6,7] Data points above 250 K have been omitted because the change in magnetization with respect to applied magnetic field is small and becomes comparable to the background. The plot thus made yields a Curie constant of $C \sim 0.01 \pm 0.0015$ K and $\Theta_p = -22 \pm 5$ K, which means that the sum of the Mn-Mn interaction is antiferromagnetic and comparable to that estimated in II-VI diluted magnetic semiconductors.[8] Knowing the effective Mn concentration $\bar{x}$, the magnetic state of the Mn ion can be inferred from the Curie constant through the expression

$$C = \frac{\mu_B^2 p_{\rm eff}^2}{3k} \frac{4}{a_0^3} \bar{x} , \tag{2}$$

where μ_B is the Bohr magneton, a_0 is the lattice constant ($\sim a_{\rm InAs}$), and $p_{\rm eff}$ is given by $g[S(S+1)]^{1/2}$ with the Landé g factor ($g = 2$) and the magnetic moment S. The expression for $p_{\rm eff}$ assumes complete quenching of the orbital angular momentum, in reasonable agreement with experiment on Mn in a variety of hosts, regardless of valence state.[9] The value of $\bar{x}$ is smaller than the atomic composition x because of the antiferromagnetic coupling between Mn ions. The ratio $\bar{x}/x$, which is not a host-material-dependent parameter, depends primarily on the

TABLE I. Atomic compositions of InMnAs films deposited on GaAs(100) with different Mn beam fluxes detected by a nude ion gauge. The relative accuracy is ±5% for each element.

Sample	T_s (°C)	Mn flux (Torr)	In	Mn	As
*R*1105	280	0.26×10^{-9}	0.98	0.014	1.0
*R*1102	300	2.1×10^{-9}	0.92	0.08	1.0
*R*1110	300	4.1×10^{-9}	0.84	0.18	0.98
*R*1111	200	4.1×10^{-9}	0.84	0.18	0.98

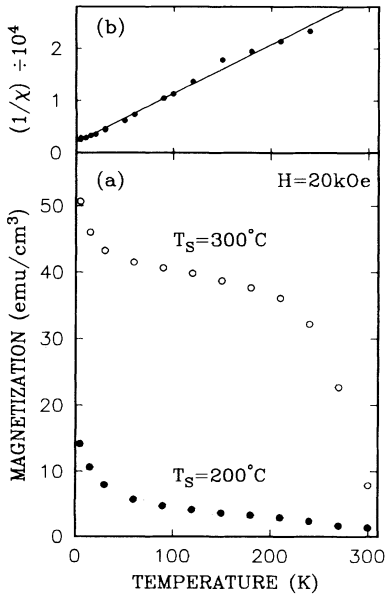

FIG. 1. (a) Temperature dependence of magnetization for samples grown at two different substrate temperatures on semi-insulating GaAs(100) substrates. (b) Plot of inverse magnetic susceptibility $1/\chi$ vs temperature T for the paramagnetic component of the sample grown at 200 °C. A straight line was obtained by the least-squares fit.

configuration of nearest-neighbor pairings and is known to be $\bar{x}/x \lesssim 0.4$ for $x > 0.1$.[10] The p_{eff} is then extracted; $p_{\text{eff}}^2 \gtrsim 37$ or $S \gtrsim 5.2/2$. Since the maximum magnetic moment is $\frac{5}{2}$ (Mn^{2+}) among Mn ions, S obtained in this fashion would indicate a valence state of Mn^{2+}. This analysis is not conclusive, however, as the ratio $\bar{x}/x$ is not strictly known. The other possibility of Mn^{3+}, for example, cannot be excluded, which may arise from a simple substitution of Mn ions for the group-III sites of In. In this case, the theoretical p_{eff} is expected to be $p_{\text{eff}}^2 \sim 24$ ($S = \frac{4}{2}$), requiring a larger value of $\bar{x}$ closer to the atomic composition x, say, $\bar{x}/x \sim 0.6$.

The $T_s = 300\,^\circ$C film exhibits a very strong magnetization up to ~ 200 K beyond which gradual reduction takes place, pointing toward an ordering temperature near 310 K. This behavior is qualitatively similar to that observed in MnAs which is known to be a ferromagnetic metal with a transition temperature of 320 K.[7] Indeed, the existence of magnetic hysteresis confirms that the sample is in a ferromagnetic state up to room temperature. The Mn composition, based on the magnetization of pure MnAs, is estimated to be roughly $x = 0.04$–0.05, so that the remaining portion of Mn is probably still in the form of a homogeneous alloy, as implied in the rise of magnetization below 20 K.

We now evaluate the films metallurgically to study the effects of Mn incorporation on crystal lattices. In Fig. 2(a), we show θ-2θ-scan data of x-ray diffraction for a (004) reflection of 2.2–2.7-μm-thick films grown at $T_s = 200\,^\circ$C on InAs(100) substrates with different Mn compositions. Measurements were performed at room temperature using a high-resolution x-ray diffractometer which utilized a highly monochromatic and well collimated beam of Cu-$K\alpha_1$ radiation produced through a nondispersive, channel-cut monochromator of Ge single crystals.[11] As seen for the case of a Mn composition of $x = 0.05$, a broad peak is superimposed on a sharp peak due to the InAs substrate. The shift of its central position to a slightly higher angle is indicative of a decrease in the lattice constant of $In_{1-x}Mn_xAs$, whereas its broadness is expected to result from fluctuations. This shift is further enhanced and becomes more pronounced with increasing Mn composition, as shown for $x = 0.18$. The peak positions, as indicated by broken arrows, are extracted by subtracting the substrate components. From linear extrapolation to $x = 1.0$, the lattice constant of a hypothetical zinc-blende MnAs is found to be $a_{\text{MnAs}} \sim 6.014$ Å.

The observed shift in lattice constants in Fig. 2(a) tends to diminish for samples grown at high temperatures. Instead, several small peaks become noticeable at $\theta \sim 25^\circ$–31°, as shown in Fig. 2(b), indicating the existence of inclusions. When measurements were performed by tilting the samples by 2° off the (001) plane, these peaks disappeared together with the main (004) reflection. Clearly, the inclusions are not randomly oriented but are aligned in a certain direction parallel to the (001) epitaxial plane to satisfy a symmetrical Bragg diffraction. The net amount of the inclusion is of the order of 10% with respect to the entire epilayer region, as estimated from the relative integrated intensities between the primary and secondary peaks. Knowing that MnAs is ferromagnetic, these secondary peaks are believed to originate from MnAs-like clusters.

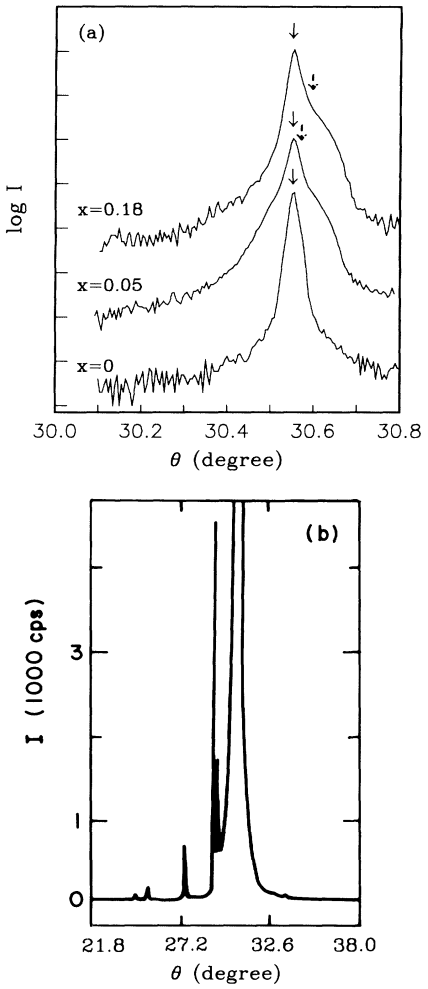

FIG. 2. (a) X-ray diffraction θ-2θ-scan data of a (004) reflection for $In_{1-x}Mn_xAs$/InAs(100) with different Mn composition x. Samples were grown at $T_s = 200\,^\circ$C. Arrows represent peak positions of both InAs substrates and InMnAs epilayers. (b) θ-2θ-scan data taken by a highly sensitive powder diffractometer for the sample grown at 280 °C with Mn composition $x = 0.05$.

The paramagnetic films exhibit properties characteristic of semiconductors. Hall measurements up to 6 kOe show a linear dependence of the Hall voltage on magnetic field and n-type conduction, the same as in the case of undoped InAs films. An anomalous Hall effect is not noticeable, which is probably reasonable because of the relatively weak contribution of magnetization in the low-field regime. Based on these measurements, the carrier

concentration and the mobility for the $x=0.18$ sample are 1.0×10^{16} cm^{-3} and 540 cm^2/V sec at 77 K, respectively. The observation of n-type conduction suggests that the Mn acceptor model ($3d^5$ plus one hole), which was valid in the doping regime,[12] may not be extended simply to the alloy system. Infrared-absorption experiments at room temperature, using Fourier-transform infrared spectroscopy, indicate that the band gaps of $In_{1-x}Mn_xAs$ are smaller than that of InAs. The absorption spectrum of $In_{0.82}Mn_{0.18}As$, for example, is shifted toward lower energy by about 50 meV.

Exploring other III-V semiconductor materials, we have found that a high concentration of Mn can also be incorporated in GaAs. The growth at $T_s=580\,^\circ$C resulted in an accumulation of Mn onto the surface, but this process was drastically suppressed at $T_s=400\,^\circ$C with the resulting films exhibiting ferromagnetic behavior. It is evident that, for both InMnAs and GaMnAs, the process toward phase separation is hindered by a lowering of the growth temperature, and the incorporation of Mn can far exceed its solubility. These results demonstrate that the diluted magnetic III-V semiconductors are in the metastable state, where the Mn atoms are inhibited from coalescing to form segregated phases.

We are grateful to A. Boulding for performing the electron microprobe analysis, H. Lilienthal and T. R. McGuire for their collaboration in the magnetic measurement, and A. Harwit for his collaboration in the infrared-absorption experiment. This work is sponsored in part by the U.S. Army Research Office.

---

[a]Permanent address: Department of Electrical Engineering, Hokkaido University, Sapporo 060, Japan.

[1]*Diluted Magnetic Semiconductors,* edited by J. K. Furdyna and J. Kossut, Semiconductor and Semimetals Vol. 25 (Academic, Boston, 1986); N. B. Brandt and V. V. Moshchalkov, Adv. Phys. **33**, 193 (1984).

[2]M. Ilegems, R. Dingle, and L. W. Rupp, Jr., J. Appl. Phys. **46**, 3059 (1975); Th. Frey, M. Maier, J. Schneider, and M. Gehrke, J. Phys. C **21**, 5539 (1988).

[3]D. G. Andrianov, V. V. Karataev, G. V. Lazareva, Yu. B. Muravlev, and A. S. Savel'ev, Fiz. Tekh. Poluprovodn **11**, 1252 (1977) [Sov. Phys. Semicond. **11**, 738 (1977)], and references within.

[4]D. DeSimone, C. E. C. Wood, and C. A. Evans, Jr., Appl. Phys. **53**, 4938 (1982).

[5]Y. Umehara and S. Koda, Metallography **7**, 313 (1974).

[6]S. von Molnar, H. Munekata, H. Ohno, and L. L. Chang (to be published).

[7]C. P. Beam and D. S. Rodbell, Phys. Rev. **126**, 104 (1962).

[8]S. B. Oseroff, Phys. Rev. B **25**, 6584 (1982).

[9]See, for example, A. H. Morrish, *The Physical Principles of Magnetism* (Wiley, New York, 1965), p. 67.

[10]Y. Shapira, S. Foner, D. H. Ridgley, K. Dwight, and A. Wold, Phys. Rev. B **30**, 4021 (1984).

[11]A. Segmüller, Adv. X-Ray Anal. **29**, 353 (1986).

[12]J. Schneider, U. Kaufmann, W. Wilkening, M. Baeumler, and F. Köhl, Phys. Rev. Lett. **59**, 240 (1987).